Narrow-line magneto-optical trap for erbium

A. Frisch,[1] K. Aikawa,[1] M. Mark,[1] A. Rietzler,[1] J. Schindler,[1] E. Zupanič,[1,2] R. Grimm,[1,3] and F. Ferlaino[1]

[1]*Institut für Experimentalphysik and Zentrum für Quantenphysik, Universität Innsbruck, Technikerstraße 25, A-6020 Innsbruck, Austria*
[2]*Jožef Stefan Institute, Jamova 39, SI-1000 Ljubljana, Slovenia*
[3]*Institut für Quantenoptik und Quanteninformation, Österreichische Akademie der Wissenschaften, A-6020 Innsbruck, Austria*

We report on the experimental realization of a robust and efficient magneto-optical trap for erbium atoms, based on a narrow cooling transition at 583 nm. We observe up to $N = 2 \times 10^8$ atoms at a temperature of about $T = 15\,\mu$K. This simple scheme provides better starting conditions for direct loading of dipole traps as compared to approaches based on the strong cooling transition alone, or on a combination of a strong and a narrow kHz transition. Our results on Er point to a general, simple, and efficient approach to laser cool samples of other lanthanide atoms (Ho, Dy, and Tm) for the production of quantum-degenerate samples.

Laser cooling of non-alkali-metal atoms has become a very active and challenging field of research. The great appeal of unconventional atomic systems for experiments on ultracold atomic quantum gases stems from the possibility of engineering complex interactions and of accessing rich atomic energy spectra. Both features are at the foundation of a number of novel and fascinating phenomena. For instance, the energy spectra of two-valence-electron species, such as alkaline-earth-metal and alkaline-earth-metal-like atoms, feature narrow and ultranarrow optical transitions, which are key ingredients for ultraprecise atomic clocks [1], efficient quantum computation schemes [2], and novel laser cooling approaches, as demonstrated in experiments with Sr, Yb, and Ca [3–5].

As a next step in complexity, multivalence-electron atoms with a non-S electronic ground state such as lanthanides are currently attracting increasing experimental and theoretical interest. Among many, one of the special features of lanthanides is the exceptionally large magnetic dipole moment of atoms in the electronic ground state (e.g., $7\mu_B$ for Er and $10\mu_B$ for both Dy and Tb), which provides a unique chance to study strongly dipolar phenomena with atoms. Highly magnetic atoms interact with each other not only via the usual contact interaction but also via an anisotropic and long-range interaction, known as the dipole-dipole interaction [6]. Chromium was the first atomic species used for experiments on atomic dipolar quantum gases [7,8], and the even more magnetic lanthanides are nowadays in the limelight thanks to laser cooling experiments on Er and Tm [9,10] and to the recent realization of quantum-degenerate Dy gases [11,12].

Similarly to Yb and the alkaline-earth-metal atoms, the atomic energy spectra of magnetic lanthanides include broad, narrow, and ultranarrow optical transitions. This collection of lines is reflected in a wide choice of possible schemes for laser cooling experiments. However, all experiments on Zeeman slowing and cooling in a magneto-optical trap (MOT) with magnetic lanthanides so far have relied on an approach that is essentially based on the strongest cycling transition [9,10,13]. This broad transition typically lies in the *blue* between 400 and 430 nm and has a linewidth on the order of few tens of MHz. As a consequence, the Doppler temperature is close to 1 mK. Such a high temperature makes direct loading

from a MOT into a dipole trap difficult and inefficient, even when sub-Doppler mechanisms take place [14,15]. To further decrease the temperature of atoms prior to the dipole trap loading, an additional MOT stage based on an ultranarrow kHz-linewidth transition was applied in Refs. [11,13], making the whole experimental procedure more involved.

Taking advantage of the rich atomic spectrum of lanthanides, we identify a different transition to be the most suitable one for MOT operation toward production of a quantum-degenerate gas. This transition, which for Er lies at 583 nm and has a linewidth of 190 kHz, represents an intermediate case between the broad (blue) and the ultranarrow (red) transitions available in the lanthanide spectra and has very similar properties to the Yb intercombination line [16,17]. Based on this narrow yellow line, we demonstrate a MOT of 2×10^8 Er atoms at a temperature as low as 15 μK. Our approach, inspired by Yb experiments [4], provides better starting conditions for direct loading into a dipole trap than the conditions achieved in other experiments with magnetic lanthanides [11].

Erbium is a heavy rare-earth element of the lanthanide series. It has six stable isotopes, among which the three bosonic isotopes ^{166}Er (34%), ^{168}Er (27%), and ^{170}Er (15%) and the fermionic isotope ^{167}Er (23%) have a high natural abundance. The Er electronic configuration is characterized by a xenonlike core, an inner open $4f$ shell, and an outer closed $6s$ shell, $[\text{Xe}]4f^{12}6s^2$. The electron vacancies in the inner f shell are a common feature of all the lanthanides (with the exception of Yb) and are at the origin of the strong magnetism as well as various interesting collisional effects [18–20].

The atomic level spectrum of Er is shown in Fig. 1. In the ground state, Er has a highly anisotropic electronic density distribution with a large orbital angular momentum $L = 5$ (H state) and a total electronic angular momentum $J = 6$. The bosonic isotopes have zero nuclear spin ($I = 0$) and consequently do not exhibit a hyperfine structure. On the contrary, the fermionic isotope ^{167}Er has a nuclear spin $I = 7/2$, leading to eight hyperfine levels, from $F = 5/2$ to $F = 19/2$, in the electronic ground state.

In Ref. [22], five different $J \rightarrow J + 1$ laser cooling transitions were identified with linewidths ranging from tens of MHz to a few Hz. Here we focus on the blue and
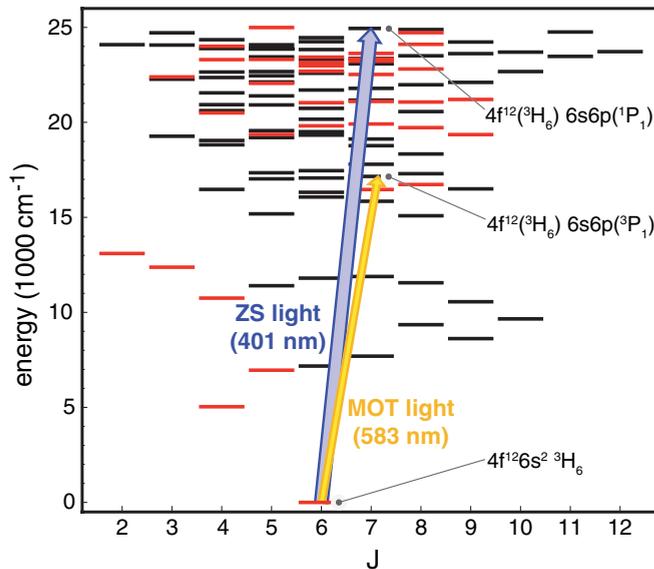
FIG. 1. (Color online) Energy levels of atomic erbium up to 25 000 cm^{-1} for different total electronic angular momentum quantum numbers J [21]. States with odd (even) parity are indicated by black (red/gray) horizontal lines. The two relevant laser cooling transitions at 401 and 583 nm are indicated by arrows [22].

the yellow transition at 401 and 583 nm, respectively; see the arrows in Fig. 1. The corresponding excited levels are the singlet $^1P_1$ and triplet $^3P_1$ states coming from the transition of an s electron into a p shell. The strong blue transition at 401 nm has a linewidth of $\Gamma_{401}/2\pi = 27.5$ MHz [23], corresponding to a Doppler temperature of $\hbar\Gamma_{401}/(2k_B) = 660\,\mu$K. We use the blue light for both Zeeman slowing and transversal cooling of the Er atomic beam. The MOT operates on the narrow yellow transition at 583 nm, which has a natural linewidth of $\Gamma_{583}/2\pi = 190$ kHz and a corresponding Doppler temperature of 4.6 μK. The line may exhibit weak leaks from the excited level into two intermediate levels with very low calculated leakage rates (0.017 and 0.0049 s^{-1}) [22]. Note that we find these losses irrelevant for all practical purposes. For ^{167}Er the hyperfine structure in the 401- and 583-nm excited states gives rise to eight levels ranging from $F' = 7/2$ to $F' = 21/2$. For the 583-nm line, the hyperfine constants are known [26]. On the contrary the hyperfine constants for the 401-nm line are currently unknown, making the operation of the fermionic MOT more challenging.

We generate the blue light from two independent blue diode lasers injection locked to a master laser. The master laser light is produced by frequency doubling methods based on a tapered amplified diode laser at 802 nm. The blue light from the master laser is locked to a hollow-cathode discharge lamp [4] via modulation transfer spectroscopy. With this setup we spectroscopically resolve the lines of the four most abundant bosonic isotopes as well as the hyperfine structure of the fermionic isotope ^{167}Er. Since the hyperfine constants of the excited level at 401 nm are unknown, we could not assign the absorption features to specific hyperfine transitions. We derive the yellow light from a dye laser operating with

Rhodamin 6G. By using an intracavity electro-optic modulator (EOM) and an external reference cavity, we stabilize the laser to a linewidth of about 50 kHz. By additionally locking the laser to an ultralow-expansion cavity, we achieve a long-term stability better than 30 kHz within a day [27].

Our experimental procedure is as follows. We load the Zeeman slowed atomic beam from an effusive, high-temperature oven directly into the narrow-line MOT. Our commercial oven typically operates at a temperature of 1300 °C, which is about 200 °C below the Er melting point. Two 3-mm apertures, separated by 50 mm, provide a geometrical collimation of the atomic beam. In addition, the atomic beam is further collimated and transversally cooled by a two-dimensional (2D) optical molasses, working on the broad 401-nm transition with a total power of about 100 mW. The beams are elliptically shaped to increase the interaction time between the atoms and the light. Thanks to the transversal cooling stage, we increase the loading flux by almost an order of magnitude.

The atomic beam then enters the Zeeman slower (ZS). Because of the limited capture velocity (a few m/s) imposed by the narrow cooling transition used for the MOT, it is crucial to design a ZS that provides enough atomic flux at low velocities [4]. We build a 360-mm-long spin-flip Zeeman slower, which can slow the atoms from 500 to about 5 m/s. The ZS light is focused at the oven position and has a total power of about 60 mW. At the MOT position, we estimate a beam diameter of about 11 mm, corresponding to an intensity of about one $I_{s,401}$, where $I_{s,401} = 56$ mW/cm^2 is the saturation intensity. Our ZS operates with light detuned by about $-20\Gamma_{401}$ (-540 MHz) from the unshifted resonance.

The narrow-line MOT is operated in a standard six-beam configuration with retroreflected beams. To increase the capture velocity of the MOT, we use large MOT beam diameters of about 30 mm. Typical MOT loading parameters include a magnetic field gradient B' (along the symmetry axis) of 4 G/cm, a laser intensity of $12I_{s,583}$ per beam with $I_{s,583} = 0.13$ mW/cm^2, and a detuning δ_{583} from the atomic transition of $-50\Gamma_{583}$ (-9.5 MHz). To measure the number of atoms in the MOT after loading, we optically compress the MOT by reducing δ_{583} to $-0.5\Gamma_{583}$ and we apply standard absorption imaging on the blue transition.

A special feature of our narrow-line MOT is the large detuning of the MOT light (typically $-50\Gamma_{583}$) needed for optimal loading. At this detuning, we observe a very strong effect of gravity on the position and shape of the atom cloud [3]. The atoms are located well below the center of the magnetic quadrupole field, and the cloud takes the form of a large semishell. To elucidate the reason for the large detuning, we monitor the loading dynamics and the lifetime of the MOT; see Fig. 2. Our measurements focus on the ^{166}Er isotope, but we have observed the same qualitative behavior also for the other isotopes.

Figure 2(a) shows the atom number in the MOT as a function of the loading time for different values of δ_{583}. We fit our data by using a standard loading rate equation [28], which includes a capture rate R and a decay rate γ; the latter accounts for both collisions between trapped atoms and collisions with the background gas. For a detuning of $-50\Gamma_{583}$ the atom number approaches its steady state in about 10 s with $N_{ss} \approx 2 \times 10^8$. For a lower value of the detuning
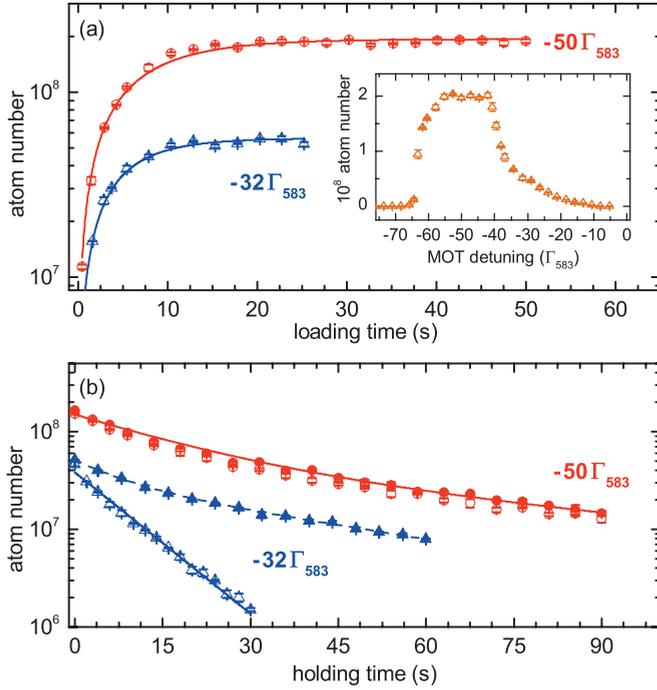
FIG. 2. (Color online) Loading (a) and decay (b) of the narrow-line MOT with ^{166}Er atoms for $\delta_{583} = -50\Gamma_{583}$ (circles) and $\delta_{583} = -32\Gamma_{583}$ (triangles). (a) Atom numbers are plotted as a function of the MOT loading time. The solid lines are fits to the data using $N(t) = N_{ss}(1 - e^{-\gamma t})$ with $N_{ss} = R/\gamma$. From the fits we obtain $\gamma = 0.137(2)$ s^{-1}, $R = 2.6(4) \times 10^{7}$ s^{-1}, and $\gamma = 0.200(4)$ s^{-1}, $R = 1.1(1) \times 10^{7}$ s^{-1} for $-50\Gamma_{583}$ and $-32\Gamma_{583}$, respectively. The inset shows the atom number after 10-s loading time as a function of the MOT detuning. (b) Atom numbers are plotted as a function of the holding time in the MOT in presence (open symbols) and absence of the ZS light (solid symbols). The solid lines are fits to the data using a double-exponential function; see text.

to $-32\Gamma_{583}$ we observe a substantial decrease of the atom number to $N_{ss} \approx 5 \times 10^{7}$. This behavior is clearly shown in the inset, where we monitor the number of atoms N_{ss} for a fixed loading time of 10 s as a function of the MOT light detuning. For detunings exceeding $\delta_{583} = -30\Gamma_{583}$ we observe a rapid increase in the atom number. When further increasing the detuning, N_{ss} first stays constant and then rapidly decreases.

We believe that the large detuning of the MOT light serves to minimize the detrimental effects of off-resonant pumping processes driven by the ZS light. According to the Zeeman shift in the quadrupole field of the MOT, we observe a spatial displacement of the atomic cloud with δ_{583} of about 1.4 mm/MHz [29]. For large detunings, this shift becomes so large that the atoms can no longer be kept in the MOT. For intermediate detunings in the range from -40 to $-55\Gamma_{583}$, the cloud displacement is advantageous for MOT operation since the atoms become spatially separated from the region of interaction with the ZS light. For small detunings, the ZS light leads to substantial losses of atoms.

The effect of the ZS light also shows up in lifetime measurements, where we monitor the number of atoms in the MOT as a function of the holding time with the ZS light being present or absent; see Fig. 2(b). For these measurements we

switch off the ZS magnetic field and the atomic beam after 10 s of MOT loading. For large detuning ($\delta_{583} = -50\Gamma_{583}$) the evolution of the atom number is not affected by the ZS light. In both cases, i.e., with the ZS light on and off, we observe faster losses in the earlier stage of the decay, which we attribute to inelastic two-body collisional processes, and a slower decay at a later time, which is finally limited by background collisions. For simplicity we use a double-exponential fit function to estimate the time constants [30]. We extract time constants of 19(3) and 80(20) s for the fast and slow dynamics, respectively. At lower MOT detuning ($-32\Gamma_{583}$), the ZS light strongly affects the decay. When the blue light is turned off, our observations are qualitatively similar to the ones at $-50\Gamma_{583}$ while with the blue light turned on the atomic loss dramatically increases. In this case the decay curve is well described by a single exponential function with a time constant $\tau = 9.0(1)$ s. This decay time is consistent with a simple estimate of pumping losses. By considering the absorption rate Γ_a of the 401-nm light at the actual intensity and detuning [31] and the branching ratio b for decay from the excited state to all the possible metastable states [9], we estimate a decay rate $1/\tau = b\Gamma_a$ of the order of 0.1 s^{-1}.

We could also demonstrate trapping of all the other Er isotopes, with the exception of the rare ^{162}Er (0.1% natural abundance). For all the bosonic isotopes we used about the same values for the detuning of the ZS and the MOT light. Figure 3(a) shows the atom number in the MOT for the different isotopes as a function of their natural abundance. For a long loading time of 20 s we observe similar atom numbers exceeding 10^{8} for the three most abundant bosonic isotopes, indicating that saturation effects might apply. For a short loading time of 5 s, the atom number increases with the natural abundance. However, we observe a more complicated
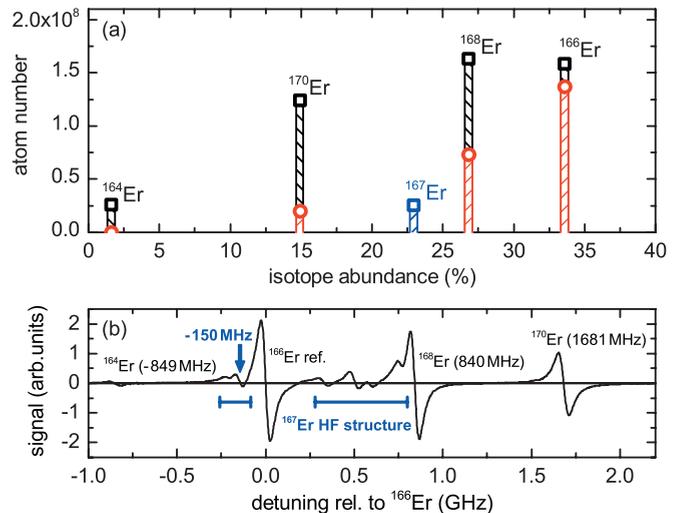

FIG. 3. (Color online) Behavior of different Er isotopes. (a) MOT atom number for the four most abundant bosonic isotopes as well as for the ^{167}Er fermionic isotope is plotted as a function of the natural abundance for 20-s (squares) and 5-s (circles) loading times. (b) Spectroscopy signal of the blue transition shows the isotope shifts for the bosonic isotopes and the HF structure of ^{167}Er. The arrow indicates the locking point used for the ZS light to produce the ^{167}Er MOT.

behavior than the expected linear growth. This might be due to slight differences in the optimal MOT parameters, but may also point to differences in scattering and collisional properties among the different isotopes.

For the fermionic isotope ^{167}Er we observe a MOT with atom number of about 3×10^7, which is substantially lower than the numbers measured for the bosonic isotopes. A simple explanation of this behavior can be that we decelerate and cool only atoms in the $F = 19/2$ hyperfine state, which has a statistical weight of about 20%. Note that a similar behavior has been observed with the fermionic ^{161}Dy MOT, which also shows lower atom numbers than the ones of bosonic MOTs [13]. An additional complication stems from the unknown hyperfine splitting of the 401-nm line. From the spectroscopic signal we could not identify *a priori* where to lock the Zeeman slower light to be resonant with the desired $F = 19/2 \rightarrow F' = 21/2$ hyperfine transition. To produce the ^{167}Er MOT, we had to proceed blindly by first locking the 583-nm MOT light on the cooling transition and then by trying different locking points for the ZS light until the MOT was visible. We finally succeed in creating a MOT by locking the ZS light to the spectroscopic line located 150 MHz below the blue transition frequency of the ^{166}Er isotope; see the arrow in Fig. 3(b).

After loading the MOT we apply a stage of compression to reduce the temperature of the atomic cloud and to achieve good starting conditions for direct loading of an optical dipole trap. With the optimized parameters $\delta_{583} = -0.5\Gamma_{583}$, $I = 0.16I_{s,583}$, and $B' = 0.8$ G/cm, we measure a temperature of 15 μK via time-of-flight experiments. In addition, Stern-Gerlach experiments indicate that atoms in the compressed MOT phase are naturally pumped in the lowest Zeeman sublevel $m_J = -6$ by the MOT light. This can be explained by considering a combined effect of the narrow cooling transition used for the MOT and of gravity. The latter pushes the atoms downward, creating an effective imbalance in the trap and leading to a preferential absorbtion of the σ^- polarized light from the lower vertical beam. For 2×10^8 atoms at $T = 15\,\mu$K we estimate a peak number density of the polarized sample of 1.5×10^{11} cm^{-3}, corresponding to a phase-space density of about 4×10^{-6}. These values are similar to the ones observed in Yb experiments using the intercombination light [4]. Compared to other experiments on magnetic lanthanides, such as Dy [11], our much simpler approach based on a single cooling light for the MOT provides higher atom numbers and similar final temperatures. We suggest that this scheme can be successfully implemented with Dy, Ho, and Tm, using the 626-nm ($\Gamma/2\pi = 135$ kHz) [32], the 598-nm ($\Gamma/2\pi = 146$ kHz) [33], and the 531-nm ($\Gamma/2\pi = 370$ kHz) [34] transitions, respectively.

In conclusion, we have demonstrated an efficient and simple approach for an Er MOT based on a single narrow-line transition. Our scheme works with all abundant Er isotopes and allows for direct loading of an optical dipole trap. In first experiments we were able to load up to 10^7 Er atoms into the dipole trap in a single focused-beam configuration. Optimization of the dipole trap loading and evaporative cooling experiments are under way in our laboratory.

[1] T. Ido and H. Katori, Phys. Rev. Lett. **91**, 053001 (2003).
[2] A. J. Daley, M. M. Boyd, J. Ye, and P. Zoller, Phys. Rev. Lett. **101**, 170504 (2008).
[3] H. Katori, T. Ido, Y. Isoya, and M. Kuwata-Gonokami, Phys. Rev. Lett. **82**, 1116 (1999).
[4] T. Kuwamoto, K. Honda, Y. Takahashi, and T. Yabuzaki, Phys. Rev. A **60**, R745 (1999).
[5] E. A. Curtis, C. W. Oates, and L. Hollberg, Phys. Rev. A **64**, 031403 (2001).
[6] T. Lahaye, C. Menotti, L. Santos, M. Lewenstein, and T. Pfau, Rep. Prog. Phys. **72**, 126401 (2009).
[7] A. Griesmaier, J. Werner, S. Hensler, J. Stuhler, and T. Pfau, Phys. Rev. Lett. **94**, 160401 (2005).
[8] Q. Beaufils, R. Chicireanu, T. Zanon, B. Laburthe-Tolra, E. Maréchal, L. Vernac, J.-C. Keller, and O. Gorceix, Phys. Rev. A **77**, 061601 (2008).
[9] J. J. McClelland and J. L. Hanssen, Phys. Rev. Lett. **96**, 143005 (2006).
[10] D. Sukachev, A. Sokolov, K. Chebakov, A. Akimov, S. Kanorsky, N. Kolachevsky, and V. Sorokin, Phys. Rev. A **82**, 011405 (2010).
[11] M. Lu, N. Q. Burdick, S. H. Youn, and B. L. Lev, Phys. Rev. Lett. **107**, 190401 (2011).
[12] M. Lu, N. Q. Burdick, and B. L. Lev, e-print arXiv:1202.4444.
[13] S. H. Youn, M. Lu, U. Ray, and B. L. Lev, Phys. Rev. A **82**, 043425 (2010).
[14] A. J. Berglund, J. L. Hanssen, and J. J. McClelland, Phys. Rev. Lett. **100**, 113002 (2008).
[15] D. Sukachev, A. Sokolov, K. Chebakov, A. Akimov, N. Kolachevsky, and V. Sorokin, JETP Lett. **92**, 703 (2010).
[16] Y. Takasu, K. Honda, K. Komori, T. Kuwamoto, M. Kumakura, Y. Takahashi, and T. Yabuzaki, Phys. Rev. Lett. **90**, 023003 (2003).
[17] Y. Takasu, K. Maki, K. Komori, T. Takano, K. Honda, M. Kumakura, T. Yabuzaki, and Y. Takahashi, Phys. Rev. Lett. **91**, 040404 (2003).
[18] R. V. Krems, G. C. Groenenboom, and A. Dalgarno, J. Phys. Chem. A **108**, 8941 (2004).
[19] C. B. Connolly, Y. S. Au, S. C. Doret, W. Ketterle, and J. M. Doyle, Phys. Rev. A **81**, 010702 (2010).
[20] S. Kotochigova and A. Petrov, Phys. Chem. Chem. Phys. **13**, 19165 (2011).

[21] Y. Ralchenko, A. Kramida, J. Reader, and N. A. Team, NIST Atomic Spectra Database, 2011.

[22] H. Y. Ban, M. Jacka, J. L. Hanssen, J. Readerand, and J. J. McClelland, Opt. Express **13**, 3185 (2005).

[23] In Ref. [24] a linewidth of $\Gamma_{401}/2\pi = 36$ MHz has been measured via fluorescence spectroscopy on atomic beams while in Ref. [25] a value of $\Gamma_{401}/2\pi = 29.5$ MHz has been obtained from lifetime measurements. We measure a linewidth of 27.5(4) MHz by using an absorption imaging technique on magneto-optically trapped atoms in the regime of low saturation parameters.

[24] J. J. McClelland, Phys. Rev. A **73**, 064502 (2006).

[25] J. E. Lawler, J.-F. Wyart, and E. A. D. Hartog, J. Phys. B **43**, 235001 (2010).

[26] W. J. Childs, L. S. Goodman, and V. Pfeufer, Phys. Rev. A **28**, 3402 (1983).

[27] Although we could clearly observe the spectroscopic signals for the different Er isotopes using a hollow-cathode lamp, we prefer to lock the 583-nm light to an ultralow-expansion cavity in order to reach higher-frequency stability.

[28] J. Weiner, V. S. Bagnato, S. Zilio, and P. S. Julienne, Rev. Mod. Phys. **71**, 1 (1999).

[29] The atomic cloud displacement Δ_x from the trap center is given by $\Delta\mu B' \Delta_x = \hbar\Delta_{583}$, where $\Delta\mu$ is the difference in magnetic moments between the ground and excited state.

[30] The standard rate equation approach is problematic, because the distorted (semishell) shape of the MOT makes it difficult to extract reliable values for the density and because the MOT may be in the high-density limit regime [28].

[31] H. J. Metcalf and P. van der Straten, *Laser Cooling and Trapping* (Springer, New York, 1999).

[32] M. Lu, S. H. Youn, and B. L. Lev, Phys. Rev. A **83**, 012510 (2011).

[33] M. Saffman and K. Mølmer, Phys. Rev. A **78**, 012336 (2008).

[34] D. Sukachev, K. Chebakov, A. Sokolov, A. Akimov, N. Kolachevsky, and V. Sorokin, Opt. Spectrosc. **111**, 633 (2011).